Lasers in Manufacturing Conference 2019

Influence of the Alloy-specific Solidification Path on the Critical Strain Rate for the Formation of Hot Cracks during Laser Beam Welding of Aluminum

Daniel Weller[a]*, Christian Hagenlocher[a], Rudolf Weber[a], Thomas Graf[a]

[a]*Institut für Strahlwerkzeuge, Pfaffenwaldring 43,70569 Stuttgart, Germany*

Abstract

The amount of the main alloying elements magnesium and silicon of a 6000 series aluminum alloy significantly determines the hot cracking susceptibility during laser beam welding. Based on the phase diagram, alloy-specific solidification paths according to Scheil can be determined. From the model of Rappaz, Drezet and Gremaud, a correlation between these alloy-specific solidification paths and the resulting critical strain rates can be derived. By experimentally determining the critical strain rates for three different AlMgSi alloys this correlation could be confirmed. This experimental proof allows aluminum alloys to be classified with regard to their susceptibility to hot cracking as a function of their characteristic solidification path.

Keywords: Laser beam welding; aluminum alloys; hot cracking susceptibility; critical strain rate; solidification path

1. Introduction

Hot cracking is one of the most frequently encountered welding defects in laser welding of high-strength aluminum alloys. Referring to Borland, 1960, hot cracks form and propagate in the last stage of the solidification when liquid is still present around the growing dendrites. Following the work of Pellini, 1952, there is a limited strain which liquid films at grain boundaries can withstand before they tear apart. The strain acting on the solidification zone depends from combined effects of metallurgical, thermal and mechanical factors, as stated by Cross, 2005.

* Corresponding author. Tel.: +49-711-685-64146; fax: +49-711-685-64146.
E-mail address: daniel.weller@ifsw.uni-stuttgart.de.

The model of Rappaz et al., 1999 relates these effects within a pressure balance to describe the susceptibility to hot cracking. A hot crack forms when the pressure drop Δp_L in the melt between the solidifying grains exceeds a critical cavitation depression Δp_c. The pressure drop Δp_L results from the thermomechanical deformation with Δp_ε and from the solidification shrinkage with Δp_{sh}, as described by Drezet and Allehaux, 2008 with

$$\Delta p_L = \Delta p_\varepsilon + \Delta p_{sh} = \frac{180\mu}{G\lambda_2^2}\left[\frac{(1+\beta)\dot{\varepsilon}}{G}\cdot A + v_T\beta \cdot B\right] \quad (1)$$

where μ is the viscosity of the melt, λ_2 the distance between the secondary dendrite arms, β the solidification shrinkage coefficient, $\dot{\varepsilon}$ the strain rate acting on the solidification zone, G the temperature gradient, and v_T the velocity of the isotherms. The two integrals

$$A = \int_{T_{coh}}^{T_L} \frac{I(T)\cdot f_S(T)^2}{(1-f_S(T))^3} dT, \quad (2)$$

$$\text{with } I(T) = \int_{T_{coh}}^{T} f_S(T)\cdot dT \quad (3)$$

$$\text{and } B = \int_{T_{coh}}^{T_L} \frac{f_S(T)^2}{(1-f_S(T))^2}\cdot dT, \quad (4)$$

each yield an alloy-specific value, which depends on the solidification path $f_s\,(T)$ of the alloy. The intervals of the integrals are set between the coherency temperature and the liquid temperature. At coherence temperature there is coalescence of the grains and volume changes due to thermomechanical deformation and solidification shrinkage can no longer be compensated by reflowing melt, referring to Feurer, 1976.

The higher the alloy-specific values of integral A and B, the higher the liquid pressure drop Δp_L and therefore the higher the risk to initiate a hot crack. Drezet and Allehaux, 2008 are using these values of the integrals A and B to classify the susceptibility to hot cracking of aluminum alloys. If Δp_L from equation (1) equals the critical cavitation depression Δp_c, a higher value of the integral A results in a lower maximum sustainable strain rate $\dot{\varepsilon}$.

This relation was experimentally investigated as described in the following by determining the maximum sustainable strain rate, which is now referred to as the critical strain rate $\dot{\varepsilon}_{crit}$.

2. Experiment

2.1. Material properties

Table 1. Amount of the main alloying elements.

Material	Mg in wt.%	Si in wt.%
6016X®	0.4	1.1
6016X®/Formalex® Remote	0.4	2.8
Ac-200 RW	0.25	3.1

The amount of silicon significantly influences the solidification path of AlMgSi alloys and with this the resulting alloy-specific values of integral A, which is now referred to as A-value. Therefore three different alloys, 6016X®, and Formalex® Remote from Constellium and Ac-200 RW from Novelis were used. This varies

the amount of silicon from 1.1 to 3.1 wt.% as listed in Table 1. Formalex® Remote was only tested in combination with 6016X®.

Fig. 1 shows as an example the solidification path of 6016X from which the belonging A-value can be calculated according to equation (2). The solidification path starts with a solid fraction of $f_s = 0$ at liquidus temperature and ends at $f_s = 1$ at solidus temperature.

The solidification paths were calculated with the software Thermo-Calc-2016b (Andersson et al., 2002 and Thermo-Calc 2018a) according to Scheil, 1942. Only the main alloy elements magnesium and silicon were taken into account. Referring to Rappaz et al., 1999 and Ludwig et al., 2005, the black line marks the solid fraction $f_{coh} = 0.94$ where the growing dendrites reach coherency.

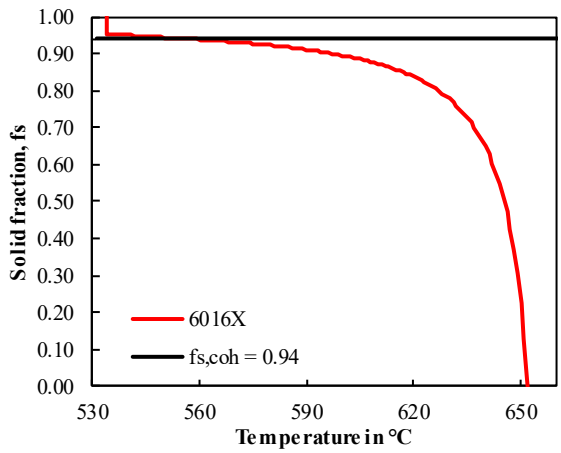

Fig. 1. Solidification path of 6016X.

2.2. Setup

To experimentally determine the critical strain rate, a self-restraint hot cracking test based on the standard (SEP 1220-3) was performed as introduced by Weller et al., 2018. In this test, the weld on the specimen is performed under an angle of 7° as shown in Fig. 2.

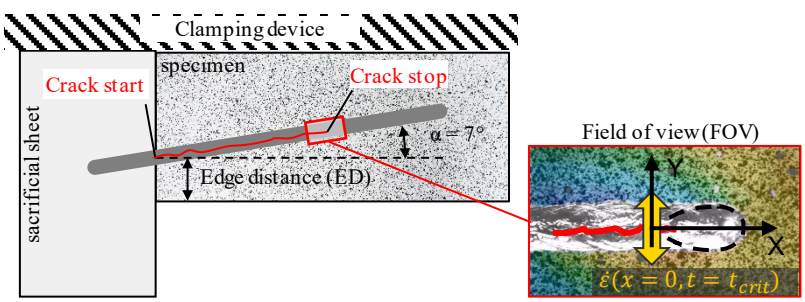

Fig. 2. Experimental Setup and a single frame from the high-speed video with the overlaid color map showing the deformation. Blue colors indicate low displacements and red colors indicate high displacements in y-direction. (according to Weller et al., 2018)

This leads to a gradually decrease of the thermomechanical load on the solidification zone. A centerline crack forms and starts to propagate as the laser process reaches the specimen. The crack propagation stops,

when a certain load limit is underrun. This load limit is quantified measuring the strain rate at the trailing edge of the melt bath, when the crack propagation stops. To determine the strain rate the displacement of a stochastic pattern applied on the surface of the specimen was tracked during welding as was introduced by Hagenlocher et al., 2018a. Therefore, a high-speed camera observed the interaction zone as marked by the red frame in Fig. 2. The red framed image section in Fig. 2 shows a single frame from the high-speed video with the overlaid color map showing the deformation transverse to the weld direction. Red colors indicate high displacements and blue colors indicate low displacements.

The same welding parameters were used for all tests so that the critical strain rate is only influenced by the alloy composition. Two sheets were welded in an overlap configuration with a laser power of $P_L = 4200\ W$ to generate welds with full penetration. The welding velocity was at *6 m/min* and the focal diameter on sample surface was at $d_f = 560\ \mu m$. To ensure steady state conditions of the welding process on the specimen, the process was started on a sacrificial sheet as shown in Fig. 2.

3. Result

Fig. 3 compares the A-values (a) with the determined critical strain rates (b) for the investigated alloys. Each value of the critical strain rates represents the average value from five measurements. The error bars each show the maximum and minimum value determined. The critical strain rates of 6016X® and the combination of 6016X® and Formalex® Remote originate from a previous publication of Hagenlocher et al., 2018b. The comparison of the two bar graphs in Fig. 3 shows that a high A-value leads to a low critical strain rate and vice versa. These results confirm the relation between the A- value and the critical strain rate, as can be derived from equation (1).

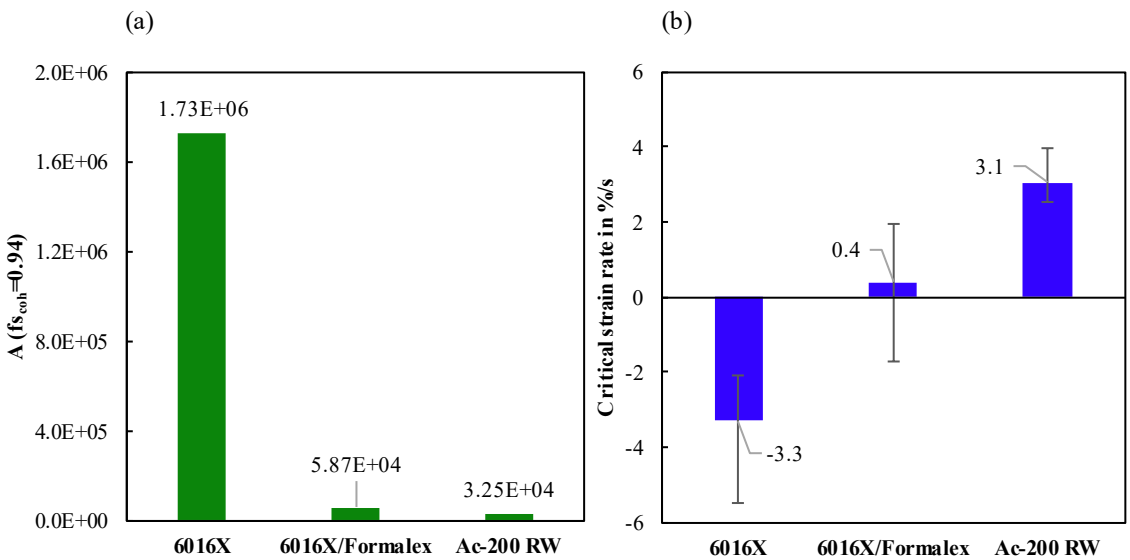

Fig. 3. (a) A-values of the investigated AlMgSi alloys calculated with $f_{coh} = 0.94$; (b) Critical strains rates of the investigated AlMgSi alloys. ($v = 6\ m/min$; $P = 4200W$, $d_f = 560\ \mu m$)

To stop the propagation of the centerline crack for the 6016X® a negative strain rate of *3.3 %/s* on the trailing edge of the melt bath and thus a compressive load is required. This indicates a high susceptibility to hot cracking and corresponds to the high A-value of *1.73E+06*. Meanwhile, the materials 6016X in

combination with Formalex® Remote and Ac-200 RW can even withstand a positive strain rate and thus a tensile load. Referring to Coniglio et al., 2008 and Ploshikhin et al., 2006, this is due to the high silicon content of these alloys, which leads to a lower susceptibility to hot cracking.

4. Summary

By experimentally determining the critical strain rates for three different AlMgSi alloys the correlation between the height of the A-value and the susceptibility to hot cracking could be shown. This experimental proof confirms the method of Drezet and Allehaux, 2008 to classify aluminum alloys by their alloy-specific A-value and thus their characteristic solidification path with regard to their susceptibility to hot cracking.

Acknowledgements

This research was funded by the Deutsche Forschungsgemeinschaft (DFG, German Research Foundation) – 389369540.

References

Andersson, J-O; Helander, Thomas; Höglund, Lars; Shi, Pingfang; Sundman, Bo, 2002. Thermo-Calc & DICTRA, computational tools for materials science, Calphad 26 2, p. 273

Borland, J. C., 1960. Generalized theory of super-solidus cracking in welds, Br. Weld. J. 7, p. 508

Coniglio, N.; Cross, C. E.; Michael, T.; Lammers, M., 2008. Defining a critical weld dilution to avoid solidification cracking in aluminum, Welding Journal 87 8, p. 237

Cross, C. E., 2005. On the origin of weld solidification cracking. In: Hot cracking phenomena in welds: Springer, p. 3

Drezet, J.-M.; Allehaux, D., 2008. Application of the Rappaz-Drezet-Gremaud Hot Tearing Criterion to Welding of Aluminium Alloys. In: Thomas Böllinghaus, Horst Herold, Carl E. Cross und John C. Lippold (Hg.): Hot Cracking Phenomena in Welds II. 1. Aufl. s.l.: Springer-Verlag, p. 27

Feurer, U., 1976. Mathematisches Modell der Warmrissneigung von binären Aluminiumlegierungen, Giesserei Forschung 28

Hagenlocher, C.; Stritt, P.; Weber, R.; Graf, T., 2018a. Strain Signatures Associated to the Formation of Hot Cracks During Laser Beam Welding of Aluminum Alloys, Optics and Lasers in Engineering 100, p. 131

Hagenlocher, Christian; Weller, Daniel; Weber, Rudolf; Graf, Thomas, 2018b. Reduction of the hot cracking susceptibility of laser beam welds in AlMgSi alloys by increasing the number of grain boundaries, Science and Technology of Welding and Joining 87 1, p. 1

Ludwig, Olivier; Drezet, Jean-Marie; Martin, Christophe L.; Suéry, Michel, 2005. Rheological behavior of Al-Cu alloys during solidification constitutive modeling, experimental identification, and numerical study, Metallurgical and Materials Transactions A 36 6, p. 1525

Pellini, William S., 1952. Strain Theory of Hot Tearing. New light on the cause of the common casting defect of hot tearing is shed by recent investigations. These indicate that hot tearing actually represents fracture through liquid films existing at near-solidus temperatures, Foundry 80, p. 125

Ploshikhin, V.; Prikhodovsky, A.; Ilin, A.; Makhutin, M.; Heimerdinger, C.; Palm, F., 2006. Influence of the weld metal chemical composition on the solidification cracking susceptibility of AA6056-T4 alloy, Welding in the World 50 11-12, p. 46

Rappaz, M.; Drezet, J.-M.; Gremaud, M., 1999. A New Hot-Tearing Criterion, Metallurgical and Materials Transactions A vol.30A, p. 449

Scheil, Erich, 1942. Bemerkungen zur Schichtkristallbildung, Zeitschrift für Metallkunde 34 3, p. 70

SEP 1220-3, 2011-08. Testing and Documentation Guideline for the Joinability of thin sheet of steel - Part 3: Laser beam welding

Thermo-Calc 2018a. TCAL5 Al-Alloys database version 5. (accessed 5th April 2019)

Weller, D.; Hagenlocher, C.; Steeb, T.; Weber, R.; Graf, T., 2018. Self-restraint hot cracking test for aluminum alloys using digital image correlation, Procedia CIRP 74C, p. 430